

- Thomason, J. F., and Iverson, N. R., 2006. Microfabric and microshear evolution in deformed till. *Quaternary Science Reviews*, **25**, 1027–1038.
- Thomason, J. F., and Iverson, N. R., 2008. A laboratory study of particle ploughing and pore-pressure feedback: a velocity-weakening mechanism for soft glacier beds. *Journal of Glaciology*, **54**, 169–181.
- Thomason, J. F., and Iverson, N. R., 2009. Deformation of the Batestown till of the Lake Michigan lobe, Laurentide ice sheet. *Journal of Glaciology*, **55**, 131–146.
- Tulaczyk, S., 1999. Ice sliding over weak, fine-grained tills: dependence of ice-till interactions on till granulometry. In Mickelson, D. M., and Attig, J. W. (eds.), *Glacial Processes: Past and Present*. Geological Society of America, Special Paper, Vol. 337, pp. 159–177.
- van der Meer, J. J. M., 1993. Microscopic evidence of subglacial deformation. *Quaternary Science Reviews*, **12**, 553–587.
- Weertman, J., 1968. Diffusion law for the dispersion of hard particles in an ice matrix that undergoes simple shear deformation. *Journal of Glaciology*, **7**, 161–165.

Cross-references

[Glaciogenic Deposits](#)
[Moraine](#)
[Quaternary Glaciation](#)
[Sediment Entrainment, Transport, and Deposition](#)
[Subglacial Processes](#)

TOPOGRAPHIC NORMALIZATION OF MULTISPECTRAL SATELLITE IMAGERY

Michael P. Bishop¹, Jeffrey D. Colby²

¹Department of Geography and Geology, University of Nebraska-Omaha, Omaha, NE, USA

²Department of Geography and Planning, Appalachian State University, Boone, NC, USA

Synonyms

Anisotropic reflectance correction; Radiometric correction

Definition

Topographic normalization of satellite imagery represents the removal/reduction of multi-scale topographic effects in satellite imagery. Surface spectral reflectance should be representative of land-surface compositional and land-cover structural variations.

Introduction

Earth scientists studying the Earth's cryosphere are increasingly making use of multispectral satellite imagery for assessing land-surface composition and properties, thematic mapping, and change detection (Bishop et al., 2004; Bishop and Shroder, 2004). The availability of new imagery and information extraction technology (i.e., algorithms and pattern recognition approaches), however, does not directly translate into obtaining accurate surface information, as image spectral variability is governed by

numerous environmental factors. Consequently, the information content in imagery varies depending upon atmospheric, topographic, surface composition, land-cover structure, and sensor characteristics that collectively determine the nature of the radiation transfer (RT) cascade at any particular location in time. These complexities often dictate the need for image preprocessing and radiometric calibration to convert calibrated digital numbers (DNs) to absolute units of at-sensor spectral radiance, and ultimately to surface spectral reflectance parameters, as many Earth science applications are primarily concerned with surface characterization.

It is widely known that topography plays a significant role in the RT cascade (Holben and Justice, 1981; Bishop and Colby, 2002). Complex topography, which includes extreme relief, steep slopes, and variations in slope azimuth (cardinal direction of slope), directly influence the amount of radiation that reaches the surface (surface irradiance). Altitude variations partially determine the magnitude of atmospheric attenuation. Other multi-scale topographic parameters, in relation to solar geometry, also cause variations in surface irradiance (e.g., shadows). The topography also governs microclimate and surface processes that control surface composition and land-cover structure. Collectively, the topography and surface composition and structure govern surface reflectance, such that the magnitude of surface reflectance varies in all directions (anisotropic reflectance). Surface reflectance is characterized by the bidirectional reflectance distribution function (BRDF). Furthermore, the topography in relation to the sensor's viewing geometry determines the BRDF sampling location, such that the magnitude of reflectance only from this BRDF location will directly propagate into the sensors field-of-view. Atmospheric attenuation and sensor characteristics then determine the magnitude of at-sensor radiance.

Clearly, the RT cascade is inherently complex, and RT interactions between the atmosphere, topography, and the surface must be taken into consideration. The influence of topography on the RT cascade dictates that satellite imagery acquired over complex terrain will exhibit spectral variability that is not representative of surface biophysical conditions. Consequently, satellite imagery frequently exhibits the *topographic effect*, which includes the presence of cast shadows, and spectral variation caused by differential illumination. It is also important to note that the influence of topography on spectral variability is not always visually detectable in imagery, as a particular topographic parameter may have varying degrees of impact on the magnitude of irradiance and reflectance. Therefore, radiometric calibration of satellite imagery requires anisotropic reflectance correction (ARC) to ensure that image reflectance variations are representative of surface-matter composition and structure, rather than indicative of atmospheric, irradiance, and topographic-induced BRDF pattern variations.

Researchers have attempted to remove the topographic effects in satellite imagery using a variety of

methodological approaches. This is generally referred to in the literature as *topographic normalization*. It should be noted, however, that topographic normalization techniques focus on removing/reducing the topographic effect in imagery, although they may not address numerous RT components influenced by topography. Consequently, topographic normalization does not represent comprehensive ARC. To our knowledge, an operational ARC model has yet to be developed to address the inherent complexities of topography and anisotropic reflectance. Therefore, we review the problem of ARC, provide simple guidelines for radiometric calibration, review various topographic normalization approaches, and assess the issues and feasibility of removing topographic effects from satellite multispectral imagery.

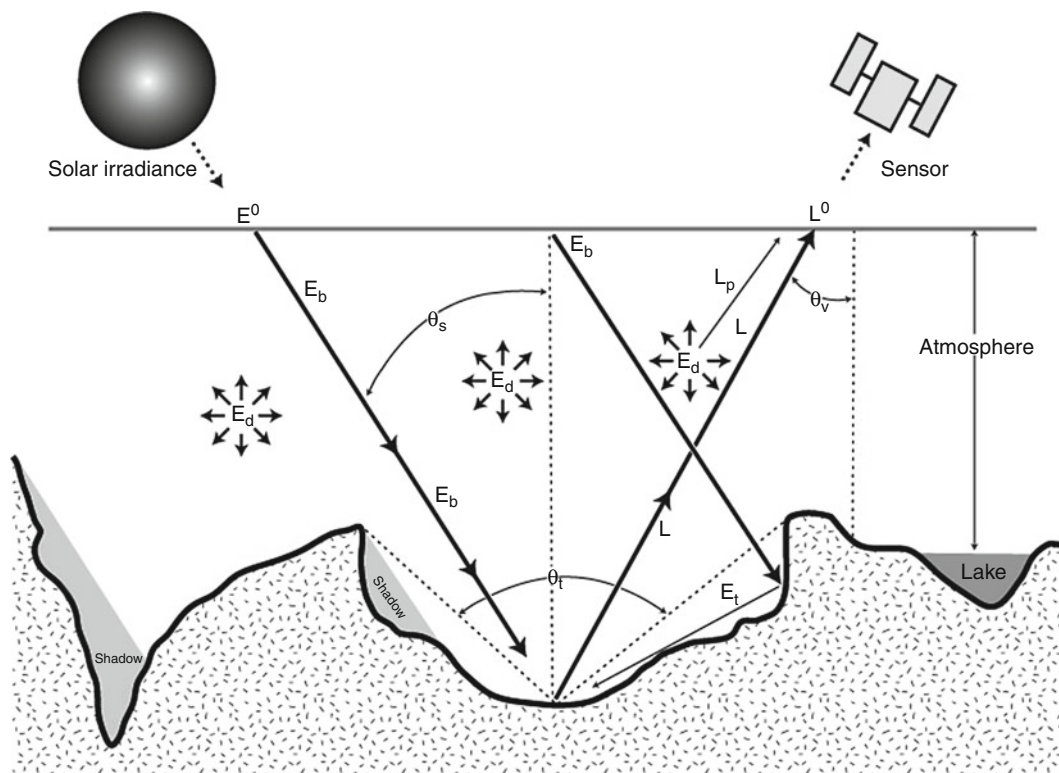
Background

Addressing the complex problem of anisotropic reflectance requires an understanding of radiation transfer processes, matter–energy interactions, and RT cascade components. Topography plays a significant role, as it has a multi-scale influence on the RT cascade. Topographic effects, however, have not been accurately characterized or systematically evaluated (Smith et al., 1980; Teillet et al., 1982; Proy et al., 1989; Bishop and Colby, 2002).

Radiation transfer

The passive reflection model of remote sensing is based upon the RT cascade from the Sun to the sensor (Figure 1). Solar irradiance variations occur at several timescales related to solar rotation, magnetic field variations, and sunspot activity. Earth's orbital variations influence the magnitude of irradiance that reaches the top of the Earth's atmosphere (exo-atmospheric irradiance, E^0) at a multitude of temporal scales. The orbital parameters of eccentricity (shape of the elliptical orbit around the Sun), obliquity (tilt of the Earth on its axis), and longitude of perihelion govern solar geometry and the distance between the Earth and the Sun. Consequently, solar and orbital parameters cause variations in the magnitude of E^0 on diurnal, annual, and longer timescales.

The exo-atmospheric irradiance is attenuated by the atmosphere, as numerous processes such as scattering, absorption, and refraction govern the magnitude of attenuation/transmission. This is controlled by atmospheric composition and the temperature/pressure vertical structure. The integrated influence of atmospheric attenuation is related to the optical depth of the atmosphere that is a function of solar geometry and landscape hypsometry (i.e., altitude distribution). Solar geometry, atmospheric, and terrain conditions are coupled to generate other sources of irradiance. Therefore, the topography strongly governs the amount of energy reaching the Earth's surface.



Topographic Normalization of Multispectral Satellite Imagery, Figure 1 Conceptual diagram of the primary radiation transfer components and multi-scale topographic effects.

Surface irradiance

The total spectral irradiance at the Earth's surface (E) is a composite of three irradiance components that are wavelength (λ) dependent such that

$$E(\lambda) = E_b(\lambda) + E_d(\lambda) + E_t(\lambda), \quad (1)$$

where E_b is the direct-beam irradiance component, E_d is the diffuse-skylight irradiance component, and E_t is the adjacent-terrain irradiance component.

The atmosphere attenuates the direct irradiance primarily by gaseous absorption and molecular and aerosol scattering (Chavez, 1996). Therefore, the downward atmospheric transmission (τ^\downarrow) is a function of the total optical depth of the atmosphere. In many mountain ranges, extreme relief dictates significant changes in τ^\downarrow over relatively short horizontal distances.

The direct irradiance is also a function of solar and terrain geometry. Local topographic conditions are represented by the incidence angle of illumination (i), such that

$$\begin{aligned} \cos i = & \cos \theta_s \cos(\beta_t) \\ & + \sin \theta_s \sin \beta_t \cos(\phi_t - \phi_s), \end{aligned} \quad (2)$$

where θ_s is the solar zenith angle, ϕ_s is the solar azimuth angle, β_t is the slope angle of the terrain, and ϕ_t is the slope-aspect angle of the terrain.

The value of $\cos i$ can be ≤ 0.0 , indicating no direct irradiance due to the orientation of the topography. The regional scale topographic relief is not accounted for by Equation 2, and the altitude distribution in the direction of ϕ_s must be considered to determine if a pixel is in shadow (S). Satellite imagery acquired in rugged terrain with relatively high, solar zenith angles and/or steep slopes exhibit cast shadows (Figure 2). The local topography and cast shadows increase the global spectral variance in satellite images, with a decrease in spectral variance associated with shadowed areas. These multi-scale topographic effects are incorporated into E_b as

$$E_b(\lambda) = E^0(\lambda)\tau^\downarrow(\lambda) \cos i S. \quad (3)$$

This component can be highly variable over complex mountain terrain.

Atmospheric scattering will produce a hemispherical source of irradiance (E_d , Figure 1). This source is composed of a direct-downward skylight component and a secondary diffuse component caused by multiple interactions between the ground surface and the atmosphere (Iqbal, 1983; Proy et al., 1989). Diffuse-skylight irradiance is influenced by hemispherical shielding of the topography, as a significant part of the hemisphere can be masked by the mesoscale relief. Consequently, only a solid angle of the sky will contribute to E_d , and this angle (θ_t) will change as a function of pixel location and direction. In general, the solid angle will increase with altitude. In mountain environments exhibiting extreme relief and deep valleys, topographic shielding of the solar diffuse irradiance can be significant (Proy et al., 1989). Mesoscale



Topographic Normalization of Multispectral Satellite Imagery, Figure 2 ASTER false-color composite (bands 3, 2, 1) depicting the Bualtar Glacier within the Hispar Mustagh region of the Karakoram Himalaya, Pakistan. This subscene exhibits extreme relief and a multitude of surface-cover types. Multi-scale topographic effects include cast shadows, local topographic effects, hemispherical shielding of the topography, and adjacent-terrain influences. Spectral variation caused by the topography is problematic for estimating surface properties and for thematic mapping applications.

topographic shielding plays less of a role in terrain exhibiting low to moderate relief.

The irradiance components E_b and E_d interact with the terrain to generate an adjacent-terrain irradiance component (E_t , Figure 1). This source of irradiance can be highly variable depending upon terrain geometry and surface composition and structure. Furthermore, the hemispherical integration of these factors, dictates the complexity of accounting for this component in mountain environments. Therefore, topographic normalization approaches do not usually account for E_t . Nevertheless, Proy et al. (1989) attempted a first-order approximation to this irradiance component assuming Lambertian reflectance (magnitude of reflectance is equal in all directions).

The contribution of E_t to the total surface irradiance in alpine environments is not accurately known, although it is generally thought to be highly variable, and significant where highly reflective rocks/sediment, vegetation, and ice/snow are prominent.

Surface reflectance

The magnitude of the reflected energy at the surface is determined by the conservation of energy, such that

$$\rho(\lambda) + \alpha(\lambda) + \tau(\lambda) = 1.0, \quad (4)$$

where, ρ , α , and τ represent reflectance, absorption, and transmission, respectively. For opaque objects ($\tau=0.0$), α is equivalent to the emissivity (ε) of the object, which describes how well the object radiates energy. The reflected surface radiance (L) can be described as

$$L(\lambda) = \rho(\lambda) \left(\frac{E(\lambda)}{\pi} \right). \quad (5)$$

Equation 5 represents isotropic reflectance (Lambertian). This assumption, however, is not valid in alpine environments due to the topography and biophysical characteristics of alpine landscapes (Smith et al., 1980; Kimes and Kirchner, 1981; Hugli and Frei, 1983; Hall et al., 1988; Dozier, 1989; Aniya et al., 1996; Greuell and de Ruyter de Wildt, 1999).

Given spatiotemporal variations in solar geometry, topography, surface composition, and land-cover structure, surface reflectance in alpine environments is highly anisotropic. It is necessary to characterize the BRDF, which describes the magnitude of reflectance for all combinations of input–output angles. For example, Greuell and de Ruyter de Wildt (1999) measured numerous BRDFs for melting glacier ice in Switzerland. They found that all BRDFs exhibited similar patterns and that the amount of anisotropy increased with an increase in wavelength, with increasing solar zenith angle, and decreasing albedo. Unfortunately, the BRDF is very difficult to accurately measure, especially on inclined surfaces, and more research is required to understand the influences associated with topography, surface-matter mixtures, and land-cover structure. This will require the development and evaluation of RT BRDF models.

The at-sensor radiance (L^0 , Figure 1) does not represent the magnitude of L , as it is attenuated by atmospheric effects governed by sensor viewing geometry and topography. Consequently, spectral variations in satellite imagery are differentially influenced by atmospheric effects, topography, and BRDF geometry variations, which are not directly related to surface-matter composition. ARC is required to address these complexities, while topographic normalization usually focuses on reducing multi-scale topographic effects related to surface irradiance. The complexity of the problem requires a special emphasis be given to radiometric calibration of satellite data before it can be utilized reliably for environmental information extraction.

The at-sensor radiance values require modification to account for the influence of the atmosphere. Numerous atmospheric-correction models for images have been developed for remote-sensing applications, and they enable the estimation of surface radiance, such that

$$L(\lambda) = \frac{(L^0(\lambda) - L_p(\lambda))}{\tau^\uparrow(\lambda, \theta_v)}, \quad (6)$$

where L_p represents the collective additive path-radiance component caused by the scattering of the direct-beam component into the sensor field-of-view, τ^\uparrow is the beam transmittance of surface reflectance through the atmosphere in the upward direction, and θ_v is the view angle of the sensor. The surface radiance must then be modified to account for topographic effects and BRDF geometry variations.

Topographic normalization

Research into topographic normalization and ARC has been ongoing for 30 years. To date, a comprehensive operational model designed to meet the needs of Earth scientists has yet to emerge. In general, scientists have taken a variety of approaches to reduce spectral variability caused by the topography. The primary approaches include the following.

Spectral feature extraction

Spectral feature extraction methods usually involve linear transformations of the original data to produce *spectral features* that enhance spectral variation related to surface conditions. Techniques such as spectral band ratioing, principal components analysis, and other methods have been shown to reduce the influence of local topographic effects (i.e., $\cos i$ and S) in satellite images (Holben and Justice, 1981; Kowalik et al., 1983; Yool et al., 1986; Walsh et al., 1990; Colby, 1991; Conese et al., 1993b; Horsch, 2003). Although such spectral features are relatively easy to generate, research has shown that local topographic effects are still present in the transformed images (Holben and Justice, 1981; Kowalik et al., 1983; Colby, 1991). The limitations of this approach are in the empirical nature of the results, such that they are scene dependent. Furthermore, there are radiometric and technical issues that must be considered.

It is important to account for atmospheric effects such as the additive path-radiance term before ratioing (Kowalik et al., 1983). This dictates that DN values must be converted to radiance and that atmospheric-correction procedures account for optical-depth variations, which are a function of altitude. In addition, information may be lost in areas where cast shadows are present, depending upon solar geometry.

One might also expect that ratioing using visible bands may not be effective due to the influence of the atmosphere. Ekstrand (1996) found this to be the case and indicated that the blue and green spectral bands of Landsat Thematic Mapper Data should not be used in ratios to

remove the topographic effect. Therefore, depending upon topographic conditions and time of image acquisition, spectral feature extraction may or may not be useful for biophysical remote sensing or thematic mapping.

Empirical approaches

Given these difficulties, empirical equations can be used to characterize the relationships between reflectance and topography within a particular scene. Normalizing equations can be generated by sampling cover types and using $\cos i$ and regression analysis (Meyer et al., 1983; Civco, 1989; Naugle and Lashlee, 1992; Ekstrand, 1996; Allen, 2000; Riano et al., 2003; Nichol et al., 2006; Wu et al., 2008).

For example, Civco (1989) used a two-stage normalization procedure that included a linear transformation based on an illumination model, and compared samples from northern and southern slopes to known areas of deciduous forest to derive an empirical wavelength-dependent calibration coefficient. In other studies, a statistical-empirical approach reportedly outperformed semi-empirical modeling (Vikhamar et al., 2004; Wu et al., 2008). It has been noted, however, that in steep and highly variable terrain, or when using imagery acquired with high solar zenith angles, empirical corrections may be less reliable (Franklin, 1991), or may not be effective at all wavelengths (Civco, 1989; Naugle and Lashlee, 1992). Empirical functions by their nature are difficult to use, as their complexity must vary to account for variations in topographic conditions (Allen, 2000).

Semi-empirical modeling

The most common approach to topographic normalization is semi-empirical modeling of the influence of topography on spectral response. Although numerous topographic parameters play a role, the parameter, $\cos i$, is considered to be the most significant and proportional to the direct irradiance. It is used in the most common algorithms as described below.

Cosine correction

Topographic effects can be reduced in imagery by accounting for the nature of surface reflectance (Lambertian or non-Lambertian) and the local topographic conditions (Colby, 1991; Ekstrand, 1996; Colby and Keating, 1998). Semi-empirical approaches make use of a digital elevation model (DEM) to account for the local illumination conditions for each pixel, and may assume isotropic upward radiance. Given the Lambertian assumption, the cosine-law correction can be used as follows:

$$L_n(\lambda) = L(\lambda) \left[\frac{\cos \theta_s}{\cos i} \right], \quad (7)$$

where L_n represents the normalized radiance.

Research indicates that this approach may produce reasonable results for terrain where slope angles and solar zenith angles are relatively low (Smith et al., 1980), although numerous investigators have found that this

approach does not work well in more complex topography, as overcorrection occurs (Figure 3), producing an inverse topographic effect (Civco, 1989; Bishop and Colby, 2002). This result can be potentially attributed to not accounting for the diffuse-skylight and adjacent-terrain irradiance components, which can significantly affect E and L (Proy et al., 1989; Trotter, 1998).

C-correction

Teillet et al. (1982) developed a semi-empirical function which is based upon linear regression such that

$$L(\lambda) = \beta \cos i + a, \quad (8)$$

where β is the slope coefficient and a is the Y-intercept of the linear relationship between L and $\cos i$. The correction



Topographic Normalization of Multispectral Satellite Imagery, Figure 3 False-color composite of normalized spectral radiance using the cosine-correction model. The influence of topography has not been removed, and extreme radiance values are generated (overcorrection) because the model does not account for irradiance from the diffuse-skylight and adjacent-terrain irradiance components.

parameter c is used to modify the cosine law as an additive term such that

$$L_n(\lambda) = L(\lambda) \left[\frac{\cos \theta_s + c}{\cos i + c} \right], \quad (9)$$

where $c = a/\beta$, and is thought to be related to the effects of indirect illumination, presumably from the diffuse-skylight irradiance and the adjacent-terrain irradiance components. It is important to note that c is not a specific physical irradiance component, because the regression analysis may also include spectral variability from atmospheric, land cover, and other multi-scale topographic effects. It does not appear to work very well in complex topography as documented in Figure 4.

Minnaert correction

The Minnaert-correction procedure has been used by a variety of investigators to reduce the topographic effect in imagery (Smith et al., 1980; Justice et al., 1981; Teillet et al., 1982; Colby, 1991; Bishop et al., 1998; Colby and Keating, 1998; Hale and Rock, 2003). The correction procedure makes use of the Minnaert coefficient k , such that

$$L_n(\lambda) = \frac{(L(\lambda) \cos e)}{(\cos^k i \cos^k e)}, \quad (10)$$

where e is the existence angle ($e = \beta_t$ for nadir viewing). As shown here, k represents a globally derived dimensionless coefficient that is wavelength dependent and ranges from 0.0 to 1.0. It is calculated using least-squares regression on the variables x and y , where $x = \log(\cos i \cos e)$ and $y = \log(L \cos e)$. The slope of the regression equation represents k . The correction procedure defaults to the Lambertian assumption when $k = 1.0$.

Although this procedure reduces the topographic effect in imagery (Figure 5), the use of one globally derived k value may not accurately characterize the variability of anisotropic reflectance caused by topography and land cover in complex environments (Bishop and Colby, 2002). Several investigators have found the use of one fixed k value to be inadequate and that a unique k value may be needed for each land-cover class in order to produce statistically significant k values (Estes, 1983; Ekstrand, 1996; Bishop and Colby, 2002).

Radiative transfer modeling

Radiation transfer processes can be mathematically characterized to account for photon flux, atmospheric and irradiance components, as well as the BRDF of surface area and volumetric mixtures of surface materials. A number of studies have recognized the importance of accounting for atmosphere-topographic coupling and the diffuse-skylight and adjacent-terrain irradiance components (Dozier, 1980; Kimes and Kirchner, 1981; Proy et al., 1989; Conese et al., 1993a; Duguay, 1993). For such modeling efforts researchers have either developed radiation transfer models (e.g., Dozier, 1980;



Topographic Normalization of Multispectral Satellite Imagery, Figure 4 False-color composite of normalized spectral radiance using the C-correction model. This model attempts to account for additional topographic variation globally, and produces better results than with the cosine-correction model. The topographic effects have been reduced, however, local topographic variation is clearly present. This demonstrates that statistical characterization via regression analysis cannot adequately account for topographic effects in complicated terrain. The values of c for ASTER VNIR spectral bands are 1.761870, 1.546854, and 1.502178, respectively.

Proy et al., 1989), or have utilized existing models such as MOTRAN (Berk et al., 1989), 6 S (Vermote et al., 1997) ATCOR (Richter, 1997, 1998), and/or GIS-based solar radiation models (Dubayah and Rich, 1995).

The difficulty in developing and applying a comprehensive physically based RT model for ARC has been noted, as a treatment of all the RT components has not been considered feasible (Hugli and Frei, 1983; Woodham and Gray, 1987; Yang and Vidal, 1990; Duguay and LeDrew, 1992). Therefore, numerous simplifying assumptions are frequently applied, including the small-angle approximation (constant solar geometry), isotropic diffuse-skylight, Lambertian reflectance, and exclusion



Topographic Normalization of Multispectral Satellite Imagery, Figure 5 False-color composite of normalized spectral radiance using the Minnaert-correction model and a global Minnaert coefficient. This model accounts for the exitance angle and anisotropic reflectance. Normalization results appear to be better than the C-correction model in some places, although the C-correction model produces better results in other places. It is clear that the topographic effect has not been effectively removed, as variation in topographic and land-cover conditions cannot be characterized by one Minnaert coefficient, and the topographic effect is evident in the imagery. Explicit modeling of multi-scale topographic effects and radiation transfer modeling are required. The values of k for ASTER VNIR spectral band are 0.214693, 0.233699, and 0.241097, respectively.

of E_t . In addition, atmospheric variables are not usually available at the time of image acquisition, and these include temperature, pressure, aerosol, water vapor, ozone, and carbon dioxide vertical profiles. Furthermore, complex surface area and volumetric mixtures of snow, ice, and mineral debris govern the anisotropic nature of the BRDF that governs E_t , and L in the direction of the sensor. Although statistical models of various RT components exist, they do not account for photon fluxes (first principles) given specific atmospheric and surface compositional mixtures.

A physically based operational ARC model requires a BRDF model based upon radiation transport theory. To our knowledge, a fully coupled ARC model that includes atmospheric, topographic, and surface RT BRDF modeling of complex mixtures in alpine environments, has yet to be developed and tested. Additional research is needed in order to better understand the relationship between the surface BRDF and topographic boundary conditions.

Issues and concerns

The complexity of the ARC problem has resulted in the dominance of empirical and semi-empirical approaches to topographic normalization. A multitude of assumptions have been utilized to address many difficult issues related to parameterization schemes and computation (Hugli and Frei, 1983). In general, the issues focus on addressing the anisotropic nature of the RT cascade, and include primary and secondary influences of topography with respect to atmospheric effects, irradiance, and surface reflectance. Furthermore, it is imperative to recognize that the numerous approaches to topographic normalization have not been systematically evaluated in terms of radiometric accuracy.

This raises concerns related to quality of data, standardization of computational methods, and approaches for evaluating normalized imagery.

Data quality

Accurate quantitative characterization of the atmosphere, topography, and surface-cover characteristics are required to determining the utility of a particular topographic normalization technique. For example, accurate geomorphometric parameters (i.e., slope angle and slope-azimuth angle) are required for each pixel, although numerous issues associated with DEM generation need to be taken into consideration. These parameters include DEM resolution, DEM source data, spatial interpolation algorithms, and geomorphometry algorithms (Justice et al., 1981; Teillet et al., 1982; Conese et al., 1993a; Pons and Sole-Sugrafies, 1994; Colby and Keating, 1998; Wu et al., 2008). Similarly, the degree of generalization associated with data collection, as governed by sensor spatial (point-spread function), spectral (spectral-response function), and radiometric characteristics may determine the influence of topography on at-sensor spectral response, and the degree to which a particular technique may reduce topographic effects. Furthermore, geometric preprocessing of satellite imagery may also influence spectral variance.

Standardization

Unfortunately, there are inconsistencies in the computation/estimation of semi-empirical model parameters. For example, a number of techniques have been used to derive the Minnaert coefficient k . In addition, different parameterization schemes are utilized. Consequently, investigators must choose from a wide variety of techniques that

have been published, without any assurances as to which approach is best suited for a particular area and topographic complexity.

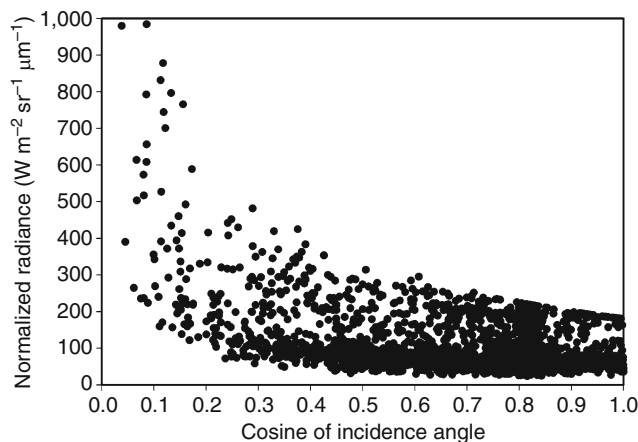
Given significant variations in landscape complexity, study area characteristics are not systematically reported to enable effective evaluation of methodological approaches. An approach may work in a particular geographic area, but may have little value in another region due to unique terrain and land-cover conditions. Investigators typically assume that their study area represents complex topography, although when compared to a standard, it is clear that there is a wide range of topographic conditions that determine whether an approach will work, as documented by others and our examples of normalized imagery. Consequently, some degree of standardization seems warranted given variations in parameterization schemes and landscape complexity. It is plausible that selected approaches/methods may be appropriate under limited conditions, although this aspect of topographic normalization has not been thoroughly investigated.

Finally, standard diagnostics to determine the ability of a method/approach to actually reduce spectral variability due to multi-scale topographic effects is sorely needed. Current diagnostic methods do not effectively address the spatial variability in spectral reflectance caused by variations in spatial, spectral, and radiometric resolution. Furthermore, data characteristics/quality and landscape complexity determine the degree to which topographic effects will manifest as spectral variation given sensor characteristics.

Image diagnostics

Normalized imagery should exhibit a global reduction in spectral variation caused by multi-scale topographic effects, and local increases in spectral variability within shadowed areas caused by land-cover variation. Unfortunately, the definition of what constitutes acceptable normalization varies by application and/or study area. The most common approach is to examine the visual appearance of imagery to determine if global spectral variation has been reduced. Very few investigators have evaluated local increases in spectral variance. Bishop and Colby (2002) have noted that topographic normalization procedures can alter the spatially dependent variance structure of satellite imagery, such that normalization may result in variance compression (loss of information) that may be visually interpreted as a reduction of topographic effects. It is extremely difficult to objectively assess the scale-dependent spectral variance in imagery via human interpretation. Furthermore, variance compression is the extreme opposite of overcorrection, as discussed in the cosine-correction section.

Another common approach has been to examine the relationship between normalized radiance and $\cos i$ (Figure 6). This approach enables the identification of statistical trends (linear or nonlinear) that may reveal overcorrection associated with lower $\cos i$ values. It is



Topographic Normalization of Multispectral Satellite Imagery, Figure 6 Relationship between normalized radiance (cosine correction of ASTER near-infrared band (0.78–0.86 μm) and the cosine of the incidence angle). The cosine-correction procedure generates a nonlinear increase in normalized radiance with decreasing values of $\cos i$. This is commonly referred to as overcorrection that is indicative of a topographic bias.

assumed that the lack of a statistical trend ($r^2 = 0.0$) is representative of good normalization and removal of topographic effects. This statistical characterization, however, does not necessarily account for topographic variation related to other multi-scale topographic effects that potentially influence atmospheric transmission, cast shadows, hemispherical shielding, and adjacent terrain and viewing geometry, as $\cos i$ only accounts for local topography. It is plausible that existing topographic effects are masked by compositional and land-cover spectral variation that can vary significantly in mountain environments. To address this would require an examination of spectral variation with altitude and the shielding coefficient, for example, although the nature of the specific relationships might also be masked by surface spectral variability.

Statistical approaches have also been traditionally used to assess the global reduction in spectral variance. Examples include basic descriptive statistics, analysis of variance, correlation analysis, and more recently, semi-variograms. These are used to demonstrate a change in spectral variance, although, with the exception of variogram analysis, these methods do not account for the spatially dependent variance structure. More importantly, however, they do not account for radiometric accuracy.

Finally, many investigators have evaluated topographic normalization techniques based upon the use of pattern recognition and classification accuracies. The assumption is that improved classification accuracies are indicative of effective normalization. This thematic mapping perspective is far removed from the notion of effective normalization of imagery to reduce topographic effects. Fundamentally, the removal of topographic effects represents a radiometric calibration issue, where the focus is

on the magnitude of surface reflectance given the BRDF. Normalization methods alter the magnitude and the spatial variability of spectral reflectance, although it is not known if the magnitude and the spatial variability are consistent with surface-matter property variation.

Thematic mapping using normalized imagery does not adequately address the issue of topographic effects and BRDF variations. Such an approach makes use of spectral variability and statistical separability in n -dimensional space, irrespective of changes in surface composition/properties.

Brute-force supervised and unsupervised classification algorithms produce thematic maps, but the classification results are also dependent upon decision rules. Consequently, classification accuracies generated from normalized imagery do not permit direct evaluation of surface reflectance and its spatial variability in terms of radiometric accuracy.

Accuracy assessment

Ultimately, it is important to better understand the anisotropic nature of the surface BRDF in mountain environments. Surface BRDF measurements are required to account for variations related to wavelength, surface composition and structure, solar geometry, and topography. Although difficult to obtain, such measurements need to be compared to radiometrically calibrated imagery (normalized imagery) to ascertain the primary and secondary topographic effects on sensor spectral response. It is also necessary to determine how well various normalization approaches generate radiometrically accurate surface reflectance values.

Without field and scale-dependent assessment of normalized imagery, it is difficult to determine the inherent advantages and disadvantages associated with various methodological approaches. Such field-based and spatial validations have yet to be established. The development and evaluation of RT BRDF models that can address the heterogeneous mixtures of surface materials typically found in mountain environments can greatly assist in better evaluating topographic normalization approaches and the production of validated surface reflectance information products.

Summary and conclusions

Understanding the complex nature of anisotropic reflection and the RT cascade in mountain environments is difficult. Multi-scale topographic effects govern numerous primary and secondary RT components. Consequently, satellite imagery contains scale-dependent spectral variation that is commonly referred to as topographic effects. The removal of spectral variation caused by topography is required to assess surface biophysical conditions and permit accurate thematic mapping. Investigators have utilized a variety of topographic normalization procedures and RT models to accomplish this, with varying degrees of success. To date, an operational model to address the difficulties of ARC has yet to emerge, given the full range of the Earth's topographic complexity.

A simplistic spatial perspective dominates most approaches, with an emphasis on direct irradiance. The nature of the problem dictates the understanding of a multitude of RT parameters in order for operational ARC of satellite imagery to be routinely conducted. This will require an explicit evaluation of time, location, matter–energy interactions, and sensor characteristics. For example, what is the influence of changing orbital parameters on irradiance and solar geometry over specific time periods, and when do these parameters need to be accurately modeled? Given the spatiotemporal variability of solar geometry, when should we not use the small-angle approximation? How does topographic complexity in relation to geographic location influence the utility of topographic normalization methods? What is the error associated with using the Lambertian assumption or statistical models of the BRDF on irradiance and reflection? To what degree does the topography influence the anisotropic nature of the BRDF? Furthermore, to what degree do sensor system characteristics determine the utility of topographic normalization methods? Many of these and other questions have not been definitively answered.

This makes it extremely difficult to determine the implications of using various topographic normalization techniques for a multitude of practical mapping applications in the Earth's cryosphere. The image ratioing method is most frequently used and is very useful for basic glacier ice and snow mapping. Very little research, however, has specifically focused on the many issues that have been previously addressed, in terms of the accuracy and validity of results needed for various alpine research and environmental concerns (e.g., water resources, mountain hazards, climate change). Clearly, more research is warranted.

Bibliography

- Allen, T., 2000. Topographic normalization of Landsat Thematic Mapper data in three mountain environments. *GeoCarto International*, **15**(2), 13–19.
- Aniya, M., Sato, H., Naruse, R., Skvarca, P., and Casassa, G., 1996. The use of satellite and airborne imagery to inventory outlet glaciers of the southern Patagonia icefield, South America. *Photogrammetric Engineering and Remote Sensing*, **62**(12), 1361–1369.
- Berk, A., Bernstein, L. S., and Robertson, D. C., 1989. MOTRAN: a moderate resolution model for LOWTRAN7. Tech. rep., Air Force Geophysical Laboratory, Hanscom AFB.
- Bishop, M. P., Barry, R. G., Bush, A. B. G., Copland, L., Dwyer, J. L., Fountain, A. G., Haeberli, W., Hall, D. K., Käab, A., Kargel, J. S., Molnia, B. F., Olsenholler, J. A., Paul, F., Raup, B. H., Shroder, J. F., Trabant, D. C., and Wessels, R., 2004. Global land-ice measurements from space (GLIMS): Remote sensing and GIS investigations of the Earth's cryosphere. *Geocarto International*, **19**(2), 57–84.
- Bishop, M. P., and Colby, J. D., 2002. Anisotropic reflectance correction of SPOT-3 HRV imagery. *International Journal of Remote Sensing*, **23**(10), 219–222.
- Bishop, M. P., and Shroder, J. F., Jr. (eds.), 2004. *Geographic Information Science and Mountain Geomorphology*. Chichester: Springer-Praxis.
- Bishop, M. P., Shroder, J. F., Jr., Sloan, V. F., Copland, L., and Colby, J. D., 1998. Remote sensing and GIS technology for

- studying lithospheric processes in a mountain environment. *Geocarto International*, **13**(4), 75–87.
- Chavez, P. S., Jr., 1996. Image-based atmospheric corrections – revisited and improved. *Photogrammetric Engineering and Remote Sensing*, **62**(9), 1025–1036.
- Civco, D. L., 1989. Topographic normalization of landsat thematic mapper digital imagery. *Photogrammetric Engineering and Remote Sensing*, **55**(9), 1303–1309.
- Colby, J. D., 1991. Topographic normalization in rugged terrain. *Photogrammetric Engineering and Remote Sensing*, **57**(5), 531–537.
- Colby, J. D., and Keating, P. L., 1998. Land cover classification using Landsat TM imagery in the tropical highlands: The influence of anisotropic reflectance. *International Journal of Remote Sensing*, **19**(8), 1459–1500.
- Conese, C., Gilabert, M. A., Maselli, F., and Bottai, L., 1993a. Topographic normalization of tm scenes through the use of an atmospheric correction method and digital terrain models. *Photogrammetric Engineering and Remote Sensing*, **59**(12), 1745–1753.
- Conese, C., Maracchi, G., and Maselli, F., 1993b. Improvement in maximum likelihood classification performance on highly rugged terrain using principal components analysis. *International Journal of Remote Sensing*, **14**(7), 1371–1382.
- Dozier, J., 1980. A clear-sky spectral solar radiation model for snow-covered mountainous terrain. *Water Resources Research*, **16**(4), 709–718.
- Dozier, J., 1989. Spectral signature of alpine snow cover from the Landsat Thematic Mapper. *Remote Sensing of Environment*, **28**, 9–22.
- Dubayah, R., and Rich, P. M., 1995. Topographic solar radiation models for GIS. *International Journal of Geographical Information Systems*, **9**(4), 405–419.
- Duguay, C. R., 1993. Radiation modeling in mountainous terrain: review and status. *Mountain Research and Development*, **13**(4), 339–357.
- Duguay, C. R., and LeDrew, E. F., 1992. Estimating surface reflectance and albedo from Landsat-5 Thematic Mapper over rugged terrain. *Photogrammetric Engineering and Remote Sensing*, **58**(5), 551–558.
- Ekstrand, S., 1996. Landsat TM-based forest damage assessment: Correction for topographic effects. *Photogrammetric Engineering and Remote Sensing*, **62**(2), 151–161.
- Estes, J. E. (ed.), 1983. *Manual of Remote Sensing*, 2nd edn. Falls Church: Sheridan, Vol. 2.
- Franklin, S. E., 1991. Image transformations in mountainous terrain and the relationship to surface patterns. *Computers and Geosciences*, **17**(8).
- Greuell, W., and de Ruyter de Wildt, M., 1999. Anisotropic reflection by melting glacier ice: measurements and parametrizations in Landsat TM bands 2 and 4. *Remote Sensing of the Environment*, **70**, 265–277.
- Hale, S. R., and Rock, B. N., 2003. Impact of topographic normalization on land-cover classification accuracy. *Photogrammetric Engineering and Remote Sensing*, **69**(7), 785–791.
- Hall, D. K., Chang, A. T. C., and Siddalingaiah, H., 1988. Reflectances of glaciers as calculated using Landsat-5 Thematic Mapper data. *Remote Sensing of Environment*, **25**, 311–321.
- Holben, B. N., and Justice, C. O., 1981. An examination of spectral band ratioing to reduce the topographic effect of remotely sensed data. *International Journal of Remote Sensing*, **2**, 115–123.
- Horsch, B., 2003. Modeling the spatial distribution of montane and subalpine forests in the central Alps using digital elevation models. *Ecological Modeling*, **168**(3), 267–282.
- Hugli, H., and Frei, W., 1983. Understanding anisotropic reflectance in mountainous terrain. *Photogrammetric Engineering and Remote Sensing*, **49**(5), 671–683.
- Iqbal, M. (ed.), 1983. *An Introduction to Solar Radiation*. New York: Academic.
- Justice, C. O., Wharton, S. W., and Holben, B. N., 1981. Application of digital terrain data to quantify and reduce the topographic effect on Landsat data. *International Journal of Remote Sensing*, **2**(3), 213–230.
- Kimes, D. S., and Kirchner, J. A., 1981. Modeling the effects of various radiant transfers in mountainous terrain on sensor response. *IEEE Transactions on Geoscience and Remote Sensing*, **19**(2), 100–108.
- Kowalik, W. S., Lyon, R. J. P., and Switzer, P., 1983. The effects of additive radiance terms on ratios of Landsat data. *Photogrammetric Engineering and Remote Sensing*, **49**(5), 659–669.
- Meyer, P., Itten, K. I., Kellenberger, T., Sandmeier, S., and Sandmeier, R., 1983. Radiometric corrections of topographically induced effects on Landsat TM data in an alpine environment. *ISPRS Journal of Photogrammetry and Remote Sensing*, **48**(4), 17–28.
- Naugle, B. I., and Lashlee, J. D., 1992. Alleviating topographic influences on land-cover classifications for mobility and combat modeling. *Photogrammetric Engineering and Remote Sensing*, **58**(8), 1217–1221.
- Nichol, J., Hang, L. K., and Sing, W. M., 2006. Empirical correction of low sun angle images in steeply sloping terrain: a slope-matching technique. *International Journal of Remote Sensing*, **27**(3).
- Pons, X., and Sole-Sugrañes, L., 1994. A simple radiometric correction model to improve automatic mapping of vegetation from multispectral satellite data. *Remote Sensing of Environment*, **48**(2).
- Proy, C., Tanre, D., and Deschamps, P. Y., 1989. Evaluation of topographic effects in remotely sensed data. *Remote Sensing of Environment*, **30**, 21–32.
- Riano, D., Chuvieco, E., Salas, J., and Aguado, I., 2003. Assessment of different topographic corrections in Landsat-TM data for mapping vegetation types. *IEEE Transactions on Geoscience and Remote Sensing*, **41**(5).
- Richter, R., 1997. Correction of atmosphere and topographic effects for high spatial resolution satellite imagery. *International Journal of Remote Sensing*, **18**(5), 1099–1111.
- Richter, R., 1998. Correction of satellite imagery over mountainous terrain. *Applied Optics*, **37**(18), 1099–1111.
- Smith, J. A., Lin, T. L., and Ranson, K. J., 1980. The Lambertian assumption and Landsat data. *Photogrammetric Engineering and Remote Sensing*, **46**(9), 1183–1189.
- Teillet, P. M., Guindon, B., and Goodenough, D. G., 1982. On the slope-aspect correction of multi-spectral scanner data. *Canadian Journal of Remote Sensing*, **8**(2), 733–741.
- Trotter, C. M., 1998. Characterising the topographic effect at red wavelengths using juvenile conifer canopies. *International Journal of Remote Sensing*, **19**(11), 2215–2221.
- Vermote, E. F., Tanré, D., Deuzé, J. L., Herman, M., and Morcrette, J., 1997. Second simulation of the satellite signal in the solar spectrum, 6 S: An overview. *IEEE Transactions on Geoscience and Remote Sensing*, **35**(3), 675–686.
- Vikhamar, D., Solberg, R., and Seidel, K., 2004. Reflectance modeling of snow-covered forest in hilly terrain. *Photogrammetric Engineering and Remote Sensing*, **70**(9).
- Walsh, S. J., Butler, D. R., Brown, D. G., and Bian, L., 1990. Cartographic modeling of snow-avalanche path location within Glacier National Park, Montana. *Photogrammetric Engineering and Remote Sensing*, **56**(5), 615–621.
- Woodham, R. J., and Gray, M. H., 1987. An analytic method for radiometric correction of satellite multispectral scanner data. *IEEE Transactions on Geoscience and Remote Sensing*, **25**(3).
- Wu, J., Bauer, M. E., Wang, D., and Manson, S. M., 2008. A comparison of illumination geometry-based methods for topographic correction of Quickbird images of an undulant area. *ISPRS Journal of Photogrammetry and Remote Sensing* **63**(2).

- Yang, C., and Vidal, A., 1990. Combination of digital elevation models with SPOT-1 HRV multispectral imagery for reflectance factor mapping. *Remote Sensing of Environment*, **32**, 35–45.
- Yool, S. R., Star, J. L., Estes, J. E., Botkin, D. B., Eckhardt, D. W., and Davis, F. W., 1986. Performance analysis of image processing algorithms for classification of natural vegetation in the mountains of Southern California. *International Journal of Remote Sensing*, **7**(5).

Cross-references

Digital Image Information Extraction Techniques for Snow Cover Mapping from Remote Sensing Data
 Mapping of Internal Glacial Layers
 Radiative Transfer Modeling
 Topographic Normalization of Multispectral Satellite Imagery

TRANSFORMATIONS OF SNOW AT THE EARTH'S SURFACE AND ITS CLIMATIC AND ENVIRONMENTAL CONSEQUENCES

Florent Domine

Laboratoire de Glaciologie et Géophysique de l'Environnement, CNRS, Saint Martin d'Hères, France

Definition

Snow crystals: Snow crystals are ice crystals formed in the atmosphere by the condensation of water vapor or the freezing of water droplets (i.e., [riming](#)).

Snow: Snow can refer either to snow crystals in the atmosphere or to snow on the ground. Here snow means snow on the ground, and the discussion is limited to [seasonal snow](#).

Transformations of snow: Because snow has a high surface-to-volume ratio, it is thermodynamically unstable and undergoes transformations at the Earth's surface. These transformations include densification, [sublimation](#), and changes in [physical properties of snow](#) such as specific surface area, [albedo](#) and thermal conductivity. Physical changes in snow are regrouped under the term [snow metamorphism](#). Transformations of snow also involve changes in the [chemical composition of snow, ice, and glaciers](#).

Introduction

When the first snow falls on the ground in autumn, it immediately creates an enormous change in the energy balance of the surface: the [albedo](#) in the visible spectral range changes from about 0.25 to about 0.95. This produces a forcing at the surface that can exceed 100 W m^{-2} , resulting in a change in the temperature of the air near the surface of several degrees at least. Another effect of this new snow is that it thermally insulates the ground from the cold autumn air, limiting its cooling (Zhang, 2005). If the first snow fall is late in season, the ground will cool more than usual, favoring the preservation of [permafrost](#). These two examples illustrate how snow can affect climate and the environment. Other examples can be found in Armstrong and Brun (2008).

After deposition to the surface, snow undergoes physical changes called metamorphism, which generates numerous types of snow crystals whose classification has been updated by Fierz et al. (2009). In the absence of liquid water, that is, if the snow remains below 0°C , [snow metamorphism](#) is caused by the transfer of water vapor between grains (Colbeck, 1982), and results in changes in snow grains sizes, shapes, and bond strength. The [physical properties of snow](#) such as albedo and thermal conductivity are affected by metamorphism, and since metamorphism is determined by climatic variables such as temperature, wind speed, and the amount of precipitation, there are some feedback loops between the transformations of snow and climate. This entry examines some of the changes undergone by snow physical properties during metamorphism and discusses a few of the relevant implications for climate and the environment.

Transformations of snow at the Earth's surface

After snow falls on the ground, a temperature gradient ∇T establishes itself between the cold atmosphere (e.g., -10°C) and the ground (e.g., 0°C), producing a gradient in the partial pressure of water vapor, $\nabla P_{\text{H}_2\text{O}}$. This gradient, in turn, causes water vapor fluxes from the base to the top of the snowpack. At the macroscopic scale, what takes place is the transfer of water vapor from the top of a crystal to the base of the overlying crystal, typically 1 mm further up (Figure 1). If the temperature gradient is greater than 20°C m^{-1} , layers of large hollow depth hoar crystals form, which have very little mechanical strength (Colbeck, 1982). If on the contrary the temperature gradient is less than a few degrees per meter, then water vapor transfer is determined mostly by the Kelvin effect, according to Equation 1

$$P_{\text{H}_2\text{O}}(r) = P_0 e^{2\gamma V_m / rRT} \quad (1)$$

where $P_{\text{H}_2\text{O}}(r)$ is the water vapor partial pressure over an ice surface of curvature r , P_0 is the water vapor partial pressure over a flat surface, γ is the ice surface tension (104 mJ m^{-2}), V_m is the molar volume of ice ($1.96 \times 10^{-5} \text{ m}^3 \text{ mol}^{-1}$), R is the gas constant, and T is the temperature in Kelvin. Shapes with a small positive radius of curvature sublimate, and the water vapor produced condenses preferentially in concave spots such as contact points between grains. In this case, cohesive snow layers of small rounded grains form (Colbeck, 1980). These two distinct dry metamorphic regimes have been discussed at length since Sommerfeld and LaChapelle (1970), who called them TG (for temperature gradient) and ET (for equi-temperature) metamorphisms. Water vapor fluxes are much more important under the TG than under the ET regime. For example, if ∇T is such that a change in temperature from -10°C to -15°C over a vertical distance of 25 cm is observed, the resulting water vapor pressure gradient will be $\nabla P_{\text{H}_2\text{O}} = 400 \text{ Pa m}^{-1}$. In comparison, under isothermal conditions, $\nabla P_{\text{H}_2\text{O}}$ can be calculated using Equation 1 for the case of a faceted crystal $400 \text{ }\mu\text{m}$ in size, and whose edges have